

The shallow magma chamber of Stromboli volcano (Italy)

D. Patanè^{1,4}, G. Barberi¹, P. De Gori², O. Cocina¹, L. Zuccarello¹, A. Garcia-Yeguas⁴, M. Castellano³, A. D'Alessandro², T. Sgroi²

¹ Istituto Nazionale di Geofisica e Vulcanologia, Sezione di Catania, Piazza Roma, 2, 95123, Catania, Italy.

² Istituto Nazionale di Geofisica e Vulcanologia, Roma, Via di Vigna Murata, 605, 00143 Roma, Italy.

³ Istituto Nazionale di Geofisica e Vulcanologia, Osservatorio Vesuviano, Via Diocleziano, 328, 80124, Napoli, Italy.

⁴ Instituto Andaluz de Geofísica, Universidad de Granada, Granada, Spain.

In this work, we integrate artificial and natural seismic sources data to obtain high-resolution images of the shallow inner structure of Stromboli volcano. Overall, we used a total of 21,953 P readings from an active seismic experiment and an additional 2,731 P and 992 S readings deriving from 269 local events. The well-defined V_p , V_s and V_p/V_s tomograms have highlighted: i) the region where magma cumulates at shallow depths (2-4 km b.s.l.), forming an elongated NE-SW high velocity body ($V_p \geq 6.0$ km/s and $V_s \geq 3.5$ km/s), with a very fast velocity core ($6.5 \leq V_p < 7.0$ km/s) of ~ 2 km³; ii) the presence of some near-vertical pipe-like structures, characterized by relatively high P-velocities values, mainly linked to past activity (e.g. Strombolicchio) and iii) a near-vertical pipe like volume with high V_p/V_s (1.78÷1.85), located beneath to the craters (down to ~ 1.0 km b.s.l.), overlying a deeper region (1.0 to 3.0 km b.s.l.) with low V_p/V_s (1.64÷1.69), interpreted as the actual and preferential pathway of magma toward the surface.

Our results demonstrate the importance of combining passive and active seismic data to improve, in a tomographic inversion, the resolution of the volcanic structures and to discover where magma may be stored.

This article has been accepted for publication and undergone full peer review but has not been through the copyediting, typesetting, pagination and proofreading process which may lead to differences between this version and the Version of Record. Please cite this article as doi: 10.1002/2017GL073008

1. Introduction

Persistently active volcanoes display a wide range of eruptive regimes that depend closely on magma dynamics and the geometry of feeding systems. Seismic tomography studies have become increasingly common over the last two decades to image and investigate the evolution of subvolcanic magmatic systems. Nonetheless, even today, we only have clues about the volcanic inner structures and the existence of magma chambers for the majority of volcanoes [e.g. *Lees, 2007*]. For basaltic volcanoes, with the exception of some well-studied volcanic edifices such as Mt. Etna [e.g. *Patanè et al., 2003, 2013*], Kilauea, and Piton de la Fournaise [*Lees, 2007*], very little is known about the shallow plumbing systems, magma chambers and conduit geometries and their relationship to eruptive behavior. Similarly, high-resolution tomographic images of storage magma regions are rare also for the andesite volcanos and only in very few cases do we have such images [e.g. *Montserrat; Paulatto et al., 2012*]. Likewise for Stromboli volcano, ITS INTERNAL STRUCTURE WAS POORLY KNOWN UNTIL NOW. For this volcano, recent petrological and geochemical studies [*Aiuppa et al., 2010; Métrich et al., 2010*] have supported the hypothesis of the presence of a shallow magmatic reservoir, located between 1-4 km below the summit, to explain the regular eruption of high-porphyrific (HP) basalts and the source origin of slugs that drive Strombolian explosions.

Stromboli is a composite volcano located in the NE part of the Aeolian Archipelago, north of Sicily (Figure 1) and has an elevated risk. It is a unique volcano, known worldwide for its persistent mild explosive activity [e.g. *Rosi et al., 2000*], defined as “Strombolian type”. Lava flows and small to large paroxysms are instead less frequent [e.g. *Andronico et al., 2008*]. The Stromboli island is the summit of a large and steep-sided edifice that rises ~ 3,000 m above the surrounding seafloor. Together with the eroded Strombolicchio edifice (STcc), the remnant of an earlier volcanic centre [*Bosman et al., 2009*] located about 1.5 km NE from the

island, and the submerged other smaller edifices (e.g. Cavoni volcano), it forms an ~ 18 km long NE-trending volcanic structure [*Bosman et al.*, 2009].

During its subaerial activity (the last 100 ka), Stromboli has undergone periods of extrusive growth and sheet intrusions, alternating with caldera formation, flank collapses and surface landsliding [*Tibaldi et al.*, 2009]. The last one occurred on December 30th 2002 along the Sciara del Fuoco (SdF), during the 2002-2003 eruptive activity, when a mass of some tens of millions of cubic meters caused a small tsunami [e.g. *Bonaccorso et al.*, 2003], fortunately during the winter season. The tsunami struck the northern coastal strip of the village of Stromboli and reached the other Aeolian Islands as well as the Sicilian and southern Italian coasts. Therefore, the main risks on this volcano are large paroxysmic eruptions that represent a potential hazard also for people living at the foot of the volcanic edifice and the tsunamis generated by subaerial and/or submarine landslides of SdF.

In recent years, Stromboli has seen an increase in its activity with lava effusions (2002-2003, 2007 and 2014), high-energy explosions (e.g. 2008, 2009), large paroxysmal eruptions (2003, 2007) and subaerial and submarine landslides generating a tsunami (2002). Increasing activity began with the eruptive crisis lasting from December 2002-July 2003 [e.g. *Bonaccorso et al.*, 2003]. Successively, there was an eruption in February-April 2007 [e.g. *Patanè et al.*, 2007] and more recently, after a longer period of modest activity, a new eruption occurred in 2014. Despite their different duration, a similar volume of magma (~ 10^7 m^3) was discharged from the vents that opened up in the SdF. Of note, were the paroxysmal explosions occurring 3 months (2002–2003) and 16 days (2007) after lava effusion during these two eruptions.

In January 2003, after the beginning of the 2002-03 eruptive crisis, the geophysical and geochemical monitoring systems of the volcano were greatly improved [*Barberi et al.*, 2009]. In particular, a new digital permanent broadband seismic network comprising 13 stations (red

triangles in Figure 1), together with several automatic systems, were installed by the Istituto Nazionale di Geofisica e Vulcanologia (INGV), in order to detect both low frequency seismic events and landslide signals [e.g. Patanè *et al.*, 2007, Barberi *et al.*, 2009].

In the frame of an INGV-Italian Civil Defense project, part of which is aimed at better understanding the internal structure of the volcano and locating magma reservoirs, the first seismic tomography experiment was undertaken at Stromboli towards the end of 2006 [Castellano *et al.*, 2008]. This in order to: i) better comprehend its activity; ii) help predict the next eruption scenario, iii) interpret the pattern of the expected precursory seismic activity and ground deformation field induced by magma upraise mechanisms in the shallow storage zones and along the feeding conduits and iv) better model edifice stability and associated hazards.

In this study, we investigate for the first time the 3D velocity structure of the subaerial and submarine portions of Stromboli volcano down to 3-4 km of depth, by integrating P- and S-wave arrival times of local seismic events and marine air-gun shots recorded during the abovementioned artificial seismic survey.

2. Data collection and inversion for the V_p , V_s and V_p/V_s structure

From the start of the third millennium, the increase of Stromboli's activity has highlighted the need to devise more suitable internal structural and velocity models of the volcano. These will allow a better understanding of the volcano's behavior both for scientific motives as well as for eventual civil defense measures.

A seismic tomography experiment (Figure 1) using airgun shots was thus undertaken at the end of 2006. A total of 1500 offshore shots were recorded by 33 inland digital three-component broadband seismic stations (13 permanent and 20 temporary) and by 10 ocean-

bottom seismometers (OBS) (Figure 1). For the very first time, the OBS deployment enabled exploring Stromboli's submarine edifice [*Marsella et al., 2007; Castellano et al., 2008*].

Since refraction seismic tomography has some limitations, as only V_p images can be retrieved, here we integrated active seismic data with a local earthquakes dataset. This strategy, performed by means of a two-step inversion, allowed assessing the structure and the plumbing system beneath the volcano. We used a total of 21,953 P readings from the active seismic experiment and an additional 2,731 P and 992 S readings deriving from 269 local events, recorded in the 2006-2007 period [*Patanè et al., 2007*] (Figure. 1). Firstly, we inverted only active seismic data by using ATOM-3D software, a modified version of the LOTOS program [*Koulakov, 2009*] designed for active source tomography. The parameterization is done with a regular grid of 9211 velocity nodes, spaced by 0.2 km both horizontally (from -15 to 15 km from the centre of island) and vertically (from 2 to -10 km of depth).

The adopted initial 1D velocity model is derived from that by *Gambino et al.* [2012], who computed a Minimum 1D P-wave velocity model to locate earthquakes in the Aeolian Archipelago, here modified in its shallow part according to *Petrosino et al.* [2002]. Since active data do not need to be relocated, the initial step is ray tracing. After travel times have been corrected for the water column, calculations are performed using the regular 3D bending ray tracer between the sources on the sea bottom and the stations, as described in *Koulakov* [2009]. Moreover, to avoid any marked influence of parametrization on the final results, we averaged the models obtained by two independent inversions carried out using two different grids with orientations of 0° and 145° .

In order to resolve the 3D V_p velocity structure beneath the Stromboli island in fine detail and to obtain the first V_s and V_p/V_s models, we then integrated active and passive seismic data and inverted the whole dataset (24,684 P and 992 S observations) by using the

tomoDDPS algorithm [Zhang *et al.*, 2009] and the input velocity model previously obtained with ATOM-3D. For this inversion an irregular grid of 841 velocity nodes has been considered, made denser in the island. Here the velocity nodes spaced 0.2 km horizontally (between -2.0 km and 2.0 km from the centre of the island) and 0.4 km vertically (between 2.0 km a.s.l. and -2.4 km b.s.l.). The grid outside of this volume is increased to 1 km and then to 2 km horizontally, while vertically it is increased to 1 km. From the visual inspection of the trade-off curve, we selected a damping value of 20 as the best compromise between the reduction of residual variance and the norm of velocity anomalies. After 9 iteration steps, a variance improvement of 42% has been obtained, reaching a final RMS of 0.169 s. Final 3D earthquake locations show hypocentral average errors of ~ 400 horizontally and ~ 500 m vertically.

Based on our data selection and inversion strategy, we obtain an improved 3D high-resolution V_p model (Figures 2 and 3) both onland and offshore. Moreover, 3D V_s and V_p/V_s models have also been obtained, albeit with a lower resolution and limited to the central part of the island (Figure 3). The reliability of these models has been validated by analyzing the complete resolution matrix (Spread Function for V_p in Figures 2 and 3) and by synthetic tests (Figures S1 to S3 in supporting information). A more detailed discussion on the reliability of these models can be found in the supporting information (see Text S1).

3. Results and discussion

In the upper 4 km of the crust (Figure 1), the dominant feature in the V_p tomograms (Figures 3 and 4) is a high velocity body (HVB; $V_p > 6.0$ km/s and $V_s > 3.5$ km/s, between -2.0 and -4.0 km of depth) in the central-north-eastern part of the island. Inside this HVB, between -3.0 and -4.0 km, a well-defined very fast velocity core ($6.5 \leq V_p < 7.0$ km/s) of ~ 2 km³ lies directly beneath the highest summit of the island in its central-southern part. Other

relatively high V_p velocity zones (3.5-4.5 km/sec) are also visible beneath the upper southern rim of the SdF just west of the active craters of the island and beneath Strombolicchio, down to ~ 1.0 km b.s.l. This latter can clearly be correlated with the magma pathway that fed the older eruptive activity and then with the changes over time of location of the intrusions [Corazzato *et al.*, 2008].

In the shallower layers of the volcanic edifice, V_p values of 2.0-3.0 km/sec (V_s of 1.0-2.0 km/sec) are consistent with highly fractured, low density materials forming the volcano deposits at the surface, in agreement with previous geophysical measurements [Chouet *et al.*, 1998; Petrosino *et al.*, 2002] and geological, volcanological and petrological observations, suggesting the presence of lavas and shallow incoherent deposits [e.g. Apuani *et al.*, 2005].

Concerning V_s and V_p/V_s tomographic images (Figure 3), there is evidence, beneath the central craters, of a relatively low V_s channel ($V_s < 2$ km/s) inclined toward the SdF and of two distinct V_p/V_s anomalous volumes. Values of $1.78 \div 1.85$ are observed down to 1 km b.s.l., changing to $1.64 \div 1.69$ at greater depth, down to ~ 3 km b.s.l. These two volumes are aligned axially with the bulk of seismicity and inclined toward the SdF, suggesting that they are part of the shallow magma conduit that feeds the present day activity of the volcano. According to laboratory experiments on igneous rocks, V_p/V_s increases are related to elevated temperatures, fractures and particularly partial melt, whereas decreases may be linked to high gas content or supercritical fluids [e.g. Mavko *et al.*, 2003].

Therefore, the shallower high V_p/V_s anomaly (low V_s zone), which defines a pipe-like structure (Figures 3 and 4) extending from the surface to ~ 1 km b.s.l., with a diameter of about 0.5 km, can be interpreted as a highly fractured and altered zone comprising the shallow magma conduit, that feeds the persistent activity of the volcano. This volume coincides with the dyke-conduit system hypothesized by modeling the long-term thermal equilibrium of the explosive system [Gilberti *et al.*, 1992], the high-frequency (1 Hz) GPS

ground deformation [Mattia *et al.*, 2004] and the source depth of VLP seismicity [e.g. Ripepe *et al.*, 2005; Chouet and Dawson, 2008]. This pipe-like structure is filled with a high-porphyric (HP) magma that feeds the Strombolian activity every few minutes [Stevenson and Blake, 1998].

Instead, the low values of V_p/V_s (1.64–1.69) can be ascribed to the combined effect of melt and gas content. This observation is consistent with the most recent geochemical and petrological studies [e.g. Allard *et al.*, 2008; Aiuppa *et al.*, 2010; Metrich *et al.*, 2010], which suggested how at the volcano-crust interface (2–4 km below the summit vents) magma may pond and CO₂-rich gas bubbles may accumulate to contents > 5 wt %. This small magmatic storage region, containing more primitive (e.g. CO₂-rich) magmas (LP magmas) represents the source zone for the gas slugs producing the regular explosive activity [e.g. Aiuppa *et al.*, 2010].

However, to better understand how the two regions of low and high V_p/V_s are connected, further investigations are needed due to the low resolution of the V_p/V_s model, especially in its deeper part.

Beyond these two anomalous V_p/V_s regions where magma can be stored, which define the shallow plumbing system, there is no evidence of a larger shallow magma accumulation zone (a large magma chamber) in the submarine part of the volcanic edifice and beneath Stromboli to ~ 4 km of depth. In fact, the HVB appears as an apparent NE-SW up-doming of the basement that shows comparable V_p values (Figure 4) and could reflect a complex of dyke/stock of past intrusions (a cooled cumulative magmatic body) along the NE-SW structural trend crossing the volcano [e.g. Corazzato *et al.*, 2008]. Prudencio *et al.* [2015] FOUND A PREFERENTIAL SCATTERING-ATTENUATION PATTERN ALONG THE SAME TREND, SUPPORTING THE PRESENCE OF THESE MAIN GEOLOGICAL HETEROGENEITIES.

These intrusions may continue into the basement with no significant velocity contrast with the basement rocks, but the tomographic images presented here highlight the internal structure of Stromboli volcano only down to a depth of ~3-4 km.

Similar high velocity anomalies, interpreted as solidified magmatic bodies in the shallower volcanic structure, have been observed under Etna [Patanè et al., 2003, 2013] and other volcanoes [Lees, 2007 and reference therein]. THESE COMMON FEATURES POINT OUT THAT SIMILAR DEPTHS OF MAGMA STORAGE ZONES ARE COMMON TO SEVERAL BASALTIC VOLCANOES INDICATING A FAVORABLE LEVEL OF MAGMA ACCUMULATION, POSSIBLY BECAUSE IT IS A LEVEL OF NEUTRAL BUOYANCY.

ACTUALLY, OUR OBSERVATIONS INDICATE THAT CURRENTLY THE MAGMAS RISE ALONG THE WESTERN BORDER OF THE HVB, IN THE REGIONS WHERE THE TWO ANOMALOUS VOLUMES OF LOW AND HIGH V_p/V_s WERE OBSERVED, BENEATH THE WESTERN FLANK OF THE VOLCANIC EDIFICE. THIS MIGHT EXPLAIN THE PROPENSITY OF THE SDF TO PRODUCE LANDSLIDES (E.G. 1930, 2002) DURING THE OPENING OF EFFUSIVE FRACTURES, DUE TO THE PRESSURE OF MAGMA IN THIS SECTOR OF THE VOLCANO. IN THE SHALLOWER PIPE-LIKE STRUCTURE (HIGH V_p/V_s), THE MAGMA BRIEFLY PONDS BEFORE ERUPTING AT THE SURFACE. CONVERSELY, THE DEEPER MAGMA ACCUMULATION ZONE (LOW V_p/V_s) MIGHT PLAY A PRIMARY ROLE IN FEEDING MAGMAS, TRIGGERING AN INCREASE OF THE STROMBOLIAN ACTIVITY OR EFFUSIVE ERUPTIONS (E.G. 2002-2003, 2007 AND 2014) OR PAROXYSMS (E.G. 2003 AND 2007).

Conclusions

By jointly inverting data of seismic local events, recorded in the 2006-2007 period, and offshore air-gun shots, recorded during the 2006 active seismic tomography experiment [Castellano et al., 2008], for the first time we have managed to build a high-resolution 3D

velocity model of Stromboli's volcanic edifice down to ca. 4 km b.s.l. Numerous tests have been performed to check the robustness of the 3D solution (see Text S1 in supporting information). In the 3D structural sketch model of Stromboli (Figure 4) we show some velocity isosurfaces at different values of V_p and V_p/V_s . The main results are summarized as follows:

- 1) The two high V_p/V_s (A in Figure 4) and low V_p/V_s (B in Figure 4) volumes beneath the central craters, reveal the position where magma is stored, the geometry of the shallow volcanic plumbing system and the reason for the different nature/types of volcanic products erupted.
- 2) The V_p isosurfaces at 3.0 km/s and 4.0 km/s (iso3 and iso4 in Figure 4), suggest the existence of some near-vertical pipe-like structures, which represent the preferential pathway of magma, probably linked to the past activity. One of these is recognizable beneath Strombolicchio (iso3 in Figure 4) and represents the plumbing system that had fed this old eruptive center. Another lies beneath the upper southern rim of the SdF (iso4 in Figure 4), just west of the active craters.
- 3) The V_p isosurface at 6.0 km/s (iso6 in Figure 4), between -2.0 and -4.0 km of depth, depicts the geometry of an almost NE-SW elongated high velocity body (HVB; iso6) inside which is a fast core (iso6.5 in Figure 4). This HVB may represent a region of cumulated old intrusions, which fed the past volcanic activity. We believe that the HVB contains a mix of dense crystals and degassed melt that could explain the high seismic velocities and almost no seismicity. Its elongation in the NE-SW direction represents, in the eastern sector of the Aeolian Archipelago, the preferential paths for magma ascent from the deep source region into the shallow reservoirs. This deep source is located in the uppermost mantle just above the Moho (9-15 km depth; Martinez-Arevalo et al., 2009).

We suggest that the regular magma supply rates of Stromboli volcano, similarly to that of other basaltic volcanoes (e.g. Etna, Piton de la Fournaise, La Réunion Island; Hawaiian volcanoes), but with differences in scale and tectonic setting, compensate for the heat loss of ascending magmas in the crust. This has enabled the growth of a large shallow magmatic volume now almost cooled beneath Stromboli, recognizable as a high seismic velocity body (HVB).

Acknowledgements The authors are grateful to the Stromboli Tomography Working Group for their support (see Author Information in *Castellano et al.*, 2008). We also thank the reviewers, J. M. Lees and anonymous for their constructive comments. H. Zhang and I. Koulakov are also thanked for providing the software TomoDDPS and ATOM-3D, respectively. The experiment has been funded by the Italian Dipartimento per la Protezione Civile (DPC-INGV Agreement 2004-2006, Projects V2-03 and V2-13). The data set used in this study to perform the tomographic inversion and the final velocity 3D models are available as supporting information (see Data Set S1 to S4).

Author Contribution D. Patanè, G. Barberi and P. De Gori have contributed equally to the study, wrote the paper and analysed data; O. Cocina, L. Zuccarello and A. Garcia-Yeguas analysed data and contributed to the discussion on the results; M. Castellano, A. D'Alessandro, T. Sgroi were involved in the study and contributed to the success of the experiment.

References

- Aiuppa, A., et al. (2010), A model of degassing for Stromboli volcano, *Earth and Planetary Science Letters*, 295, 195-204.
- Allard, P., et al. (2008), Crater gas emissions and the magma feeding system of Stromboli volcano, In: *The Stromboli volcano: An integrated study of the 2002-2003 eruption*, edited by: S. Calvari, S. Inguaggiato, M. Ripepe, M. Rosi, (Eds), AGU Geophys. Monograph. Series, Washington DC, 182, 65-80.
- Andronico, D., et al. (2008), Characterizing high energy explosive eruptions at Stromboli volcano using multidisciplinary data: An example from the 9 January 2005 explosion, *J. Volcanol. Geotherm. Res.*, 176, 541-550.
- Apuani, T., et al. (2005), Stability of a collapsing volcano (Stromboli, Italy): Limit equilibrium analysis and numerical modeling, *J. Volcanol. Geotherm. Res.*, 144, 191-210.
- Barberi, F., et al. (2009). Chronology of the 2007 eruption of Stromboli and the activity of the Scientific Synthesis Group. *J. Volcanol. Geotherm. Res.* 182, 123–130.
- Bonaccorso, A., et al. (2003), Dynamics of the December 2002 flank failure and tsunami at Stromboli volcano inferred by volcanological and geophysical observations, *Geophys. Res. Lett.*, 30, 1941, doi:10.1029/2003GL017702.
- Bosman, A., F.L. Chiocci, and C. Romagnoli (2009), Morpho-structural setting of Stromboli volcano revealed by high-resolution bathymetry and backscatter data of its submarine portions, *Bull. Volcanol.*, 71, 1007, doi:10.1007/s00445-009-0279-5.
- Caló, M., et al. (2009), Local earthquake tomography in the southern Tyrrhenian region of Italy: geophysical and petrological inferences on the subducting lithosphere, *In Subduction Zone Geodynamics*, S. Lallemand, F. Funiciello, (Eds), *Frontiers in Earth Sciences*, Springer, 85.
- Castellano, M., et al. (2008), Seismic tomography experiment at Italy's Stromboli Volcano, *Eos Trans. AGU*, 89, 269–270.
- Chouet, B. and P. Dawson (2008), Upper conduit structure and explosion dynamic at Stromboli, In: *The Stromboli volcano*, edited by: S. Calvari, S. Inguaggiato, G. Puglisi, M. Ripepe, M. Rosi, (Eds), AGU Geophys. Monograph. Series, Washington, DC, 182, 81-92.

- Corazzato, C., et al. (2008), What controls sheet intrusion in volcanoes? Structure and petrology of the Stromboli sheet complex, Italy, *J. Volcanol. Geotherm. Res.*, 173, 26-54.
- Eberhart-Phillips, D., and M. Reyners (1997), Continental subduction and three-dimensional crustal structure: The northern South Island, New Zealand, *Geophys. J. Int.*, 102, 11843-11861.
- Giberti, G., C. Jaupart, and G. Sartoris (1992), Steady-state operation of Stromboli volcano, Italy: Constraints on the feeding system, *Bull. Volcanol.*, 54, 535-541.
- Haslinger, F., et al. (1999), 3-D crustal structure from local earthquake tomography around the Gulf of Arta (Ionian region, NW Greece), *Tectonophysics*, 304, 201-218.
- Koulakov, I. (2009), Lotos code for local earthquake tomographic inversion: Benchmarks for testing tomographic algorithms, *Bull. Seism. Soc. Am.*, 99, 194-214, doi: 10.1785/0120080013.
- Lees, J.M. (2007), Seismic tomography of magmatic systems, *J. Volcanol. Geotherm. Res.*, 167, 37-56.
- Marsella, E., et al. (2007), The Stromboli geophysical experiment, *ISMAR Bologna Technical Report N.102*, 85 pp., (Available at http://projects.bo.ismar.cnr.it/MEDITERRANEAN/STROMBOLI/STR06_REP)
- Martinez-Arevalo, C., C. Musumeci, and D. Patanè (2009), Evidence of a partial melt zone beneath Stromboli volcano (Italy) from inversion of teleseismic receiver functions, *Terra Nova*, 21, 386-392.
- Mattia, M., et al. (2004), The shallow plumbing system of Stromboli Island as imaged from 1 Hz instantaneous GPS positions, *Geophys. Res. Lett.*, 31, L24610, doi:10.1029/2004GL021281.
- Mavko, G., T. Mukerji, and J. Dvorkin (2003), The Rock Physics Handbook: Tools for Seismic Analysis of Porous Media, *Cambridge University Press, New York*, 339 pp.
- Métrich, N., A., Bertagnini, and A. Di Muro (2010), Conditions of magma storage, degassing and ascent at Stromboli: new insights into the volcano plumbing system with inferences on the eruptive dynamics, *Journal of Petrology*, 51, 603-626.
- Michellini, A., and T.V. McEvelly (1991), Seismological studies at Parkfield, I, simultaneous inversion for velocity structure and hypocentres using cubic b-splines parameterization, *Bull. Seismol. Soc. Am.*, 81, 524-552.
- Patanè, D., et al. (2003), Magma ascent and the pressurization of Mount Etna's volcanic system, *Science*, 299, 2061-2063.

- Patane`, D., et al. (2007), Insights into the dynamic processes of the 2007 Stromboli eruption and possible meteorological influences on the magmatic system, *Geophys. Res. Lett.*, *34*, L22309, doi:10.1029/2007GL031730.
- Patanè, D., et al. (2013), Insights into magma and fluid transfer at Mount Etna by a multiparametric approach: A model of the events leading to the 2011 eruptive cycle, *J. Geophys. Res.*, *118*, 1-21, doi:10.1002/jgrb.50248.
- Paulatto, M., et al. (2012), Magma chamber properties from integrated seismic tomography and thermal modelling at Montserrat, *Geochemistry Geophysics Geosystems*, *13*, 26-54.
- Prudencio, J., et al. (2015), Two-dimensional seismic attenuation images of Stromboli island using active data, *Geophys. Res. Lett.*, *42*, 1717–1724, doi:10.1002/2015GL063293.
- Petrosino, S., et al. (2002), Seismic Attenuation and Shallow Velocity Structures at Stromboli Volcano, Italy, *Bull. Seism. Soc. Am.*, *92*, 1102,1116.
- Ripepe, M., A.J. Harris, E. Marchetti (2005), Coupled thermal oscillations in explosive activity at different craters of Stromboli volcano, *Geophys. Res. Lett.*, *32*, L17302, <http://dx.doi.org/10.1029/2005GL022711>.
- Rosi, M., A. Bertagnini, and P. Landi, (2000), Onset of the persistent activity at Stromboli volcano (Italy), *Bull. Volcanol.*, *62*, 294-300.
- Stevenson, D.S., and S. Blake (1998), Modelling the dynamics and thermodynamics of volcanic degassing, *Bull. Volcanol.*, *60*, 307-317.
- Tibaldi, A., et al. (2009), Subaerial-submarine evidence of structures feeding magma to Stromboli volcano, Italy, and relations with edifice flank failure and creep, *Tectonophysics*, *469*, 112-136.
- Thurber, C.H. (1993), Local earthquake tomography: velocity and Vp/Vs theory, *In Seismic Tomography: Theory and Practice*, H. M. Iyer, K. Hirahara, (Eds) (Chapman and Hall, London, 1993), 563-583.
- Toomey, D.R., and G.R. Foulger (1989), Tomographic inversion of local earthquake data from the Hengill-Grensdalur central volcano complex, Iceland, *J. Geophys. Res.*, *94*, 17497-17510.
- Zhao, D., A. Hasegawa, and H. Kanamori (1992), Tomographic imaging of P and S wave velocity structure beneath northeastern Japan, *J. Geophys. Res.*, *97*, 19909-19928.
- Zhang, H., C. Thurber, and P. Bedrosian (2009), Joint inversion for Vp, Vs, and Vp/Vs at SAFOD, Parkfield, California, *Geochemistry Geophysics Geosystems*, *10*, Q11002, doi:10.1029/2009GC002709.

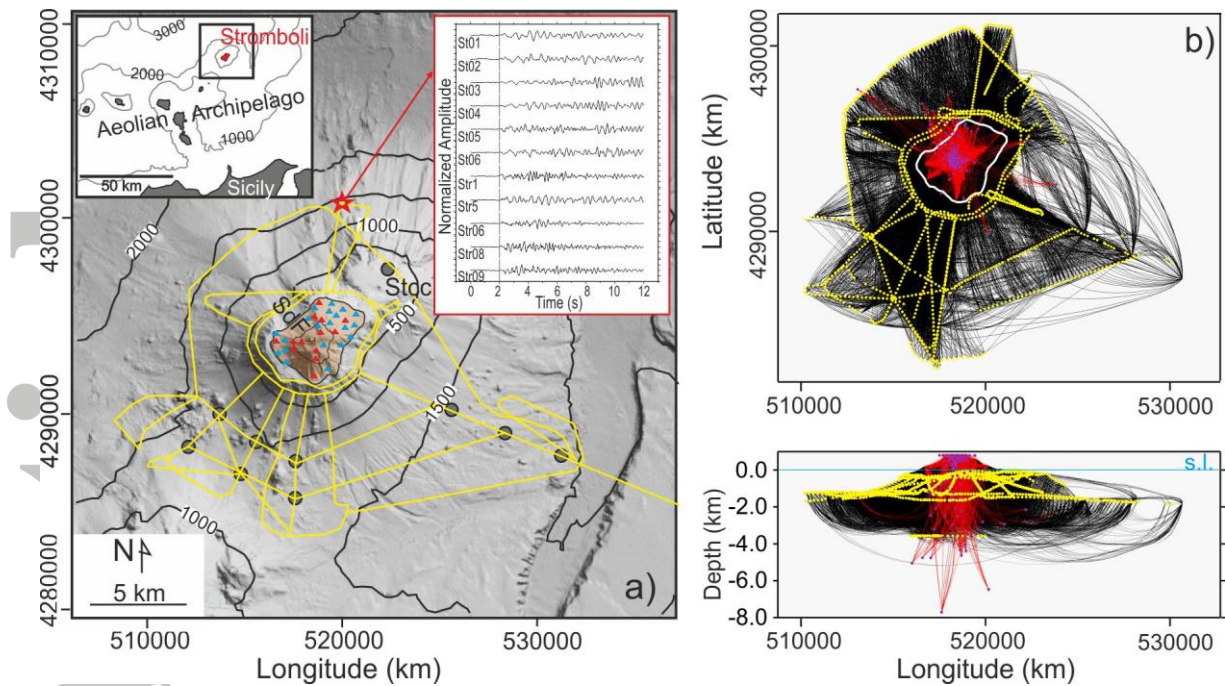


Figure 1. (left, a) Map of Stromboli volcano topography and bathymetry [Bosman *et al.*, 2009]. Recording systems and shot lines (yellow lines) during the 2006 experiment are reported. The shots done at 6 m b.s.l. were scheduled at 2-minute intervals corresponding to shot spacing of 250 meters. The red and light blue triangles on the emerged part of Stromboli indicate the 13 permanent and 20 temporary broad-band seismic stations, respectively. The dark grey circles shown the location of the 10 ocean-bottom seismometers. Some recordings of a shot are shown in the inset. The signals are filtered in the 5- to 20-hertz band. (right, b) Map and W-E cross section of P-wave ray tracing used for the inversion of the 21,953 P readings from the active seismic experiment (black lines) and of additional 2,731 P readings (red lines) from 269 selected seismic events, recorded during the 2006-2007 time span by the permanent network. The 1D earthquake locations (purple circles) and the shots (yellow circles) are also shown.

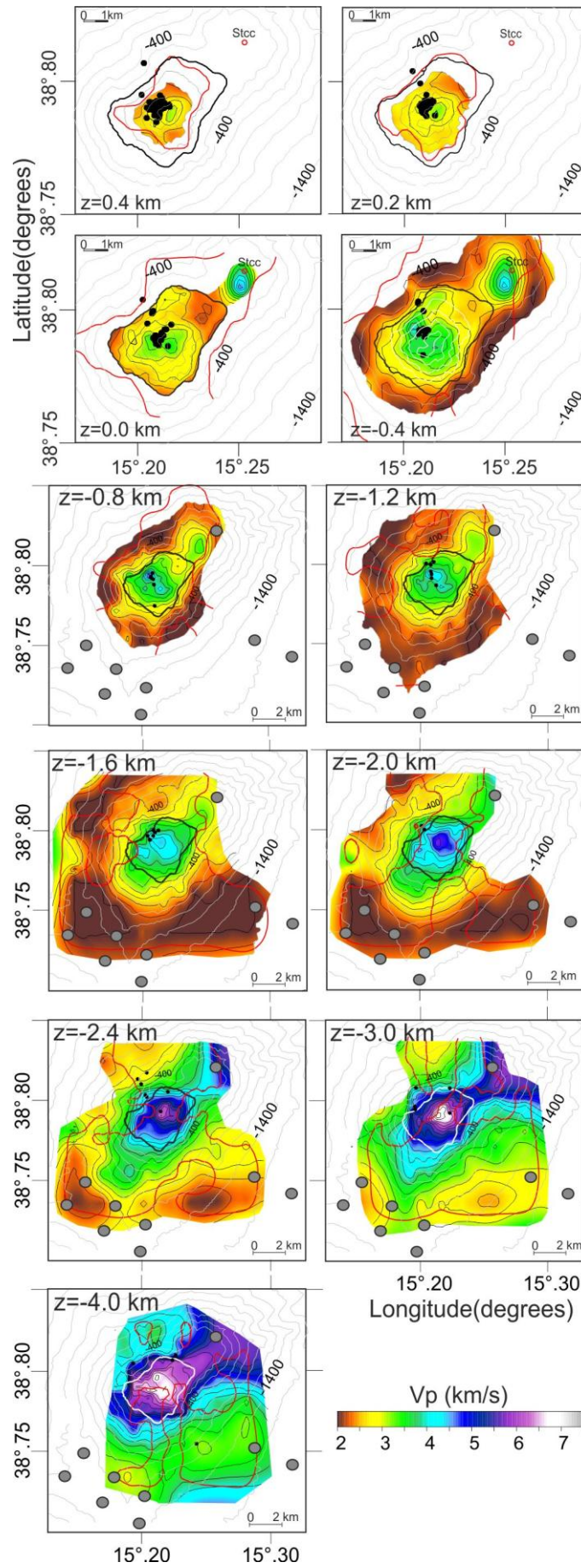


Figure 2. V_p velocity model in the well-resolved layers (from -0.4 to 3.0 km). The red lines contoured the regions of the model with $SF \leq 2$ where the resolution is good (see supplementary information for more details). The grey lines are the elevation isolines (every 200 m). The black dots in the V_p model are the relocated events with the 3D velocity model obtained here.

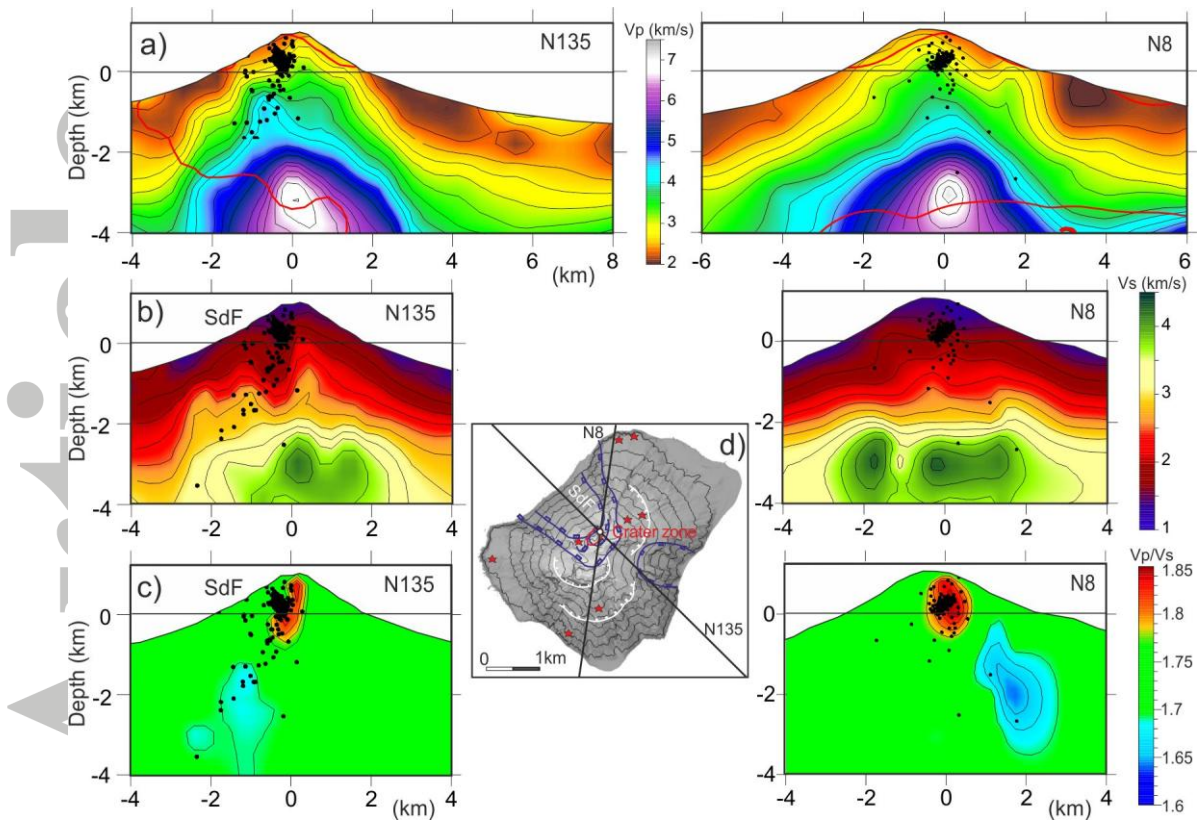


Figure 3. N135°E and N8°E cross-sections (black lines crossing the active craters in the DEM map) of the V_p , V_s and V_p/V_s models. The red lines in the V_p cross sections indicate the $SF = 2$. The black dots show the relocated events. Main lateral collapse scars (blue lines), caldera collapse rims (white lines) and eruptive vents (red stars) are shown in the island map.

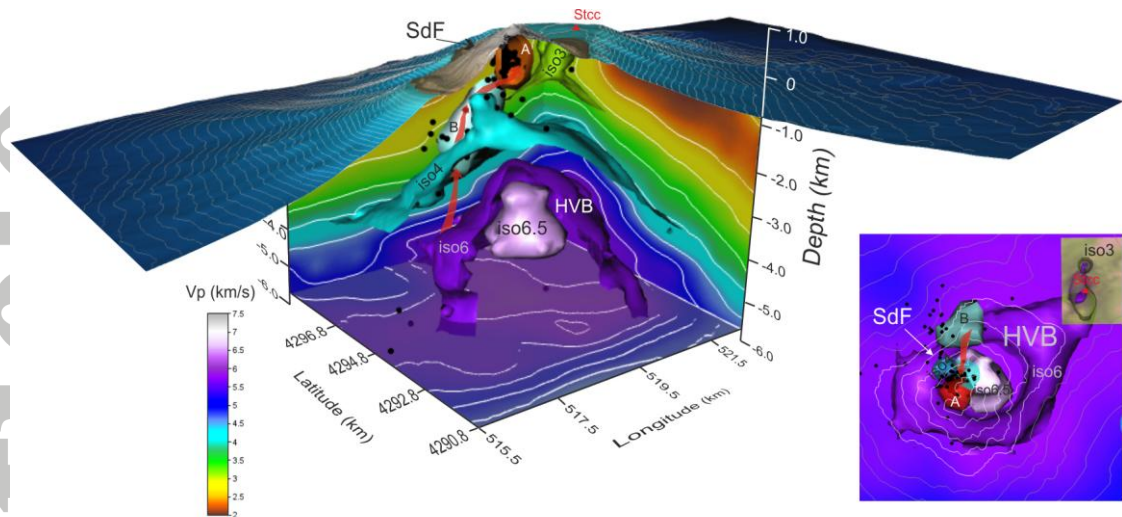


Figure 4. 3D structural sketch model of Stromboli showing: (1) Vp isosurfaces at 6.0 km/s (iso6) of the high velocity body (HVB) and the fast core inside it (iso6.5); (2) Vp isosurfaces at 4.0 km/s (iso4) and at 3.0 km/s (iso3); the latter correlated with the plumbing system feeding the old eruptive center of Strombolicchio (Stcc); (3) the high Vp/Vs shallow volume (A) and the deeper low Vp/Vs volume (B), defining the present magma pathway (red arrows). The seismicity recorded during the 2006-2007 period is also shown (black dots), evidencing how the events are mainly located to the west of the HVB. In the map on the right, the planar geometry of the HVB (iso6) is shown together with part of the others Vp isosurfaces (iso3, iso4, iso6.5) and the two high and low Vp/Vs anomalous volumes (A and B).